A NUMERICAL MODEL FOR CHARACTERIZATION OF SPECIMENS IN A MICROWAVE CAVITY

Jian-She Wang and Nathan Ida

Department of Electrical Engineering
The University of Akron
Akron, OH 44325, U.S.A.

INTRODUCTION

When a specimen is inserted in an electromagnetic cavity, the specimen causes shifts in the resonant frequencies, and also in the Q-factors if losses are considered. While these shifts can be measured via reliable methods, certain information about the specimen, such as the material properties, sizes, and possible defects, can be inferred. In this sense, one can actually characterize a material by its intrinsic resonant frequencies and Q-factors in an electromagnetic cavity. In practice, an electromagnetic cavity operates at some finite number of modes (usually the lowest modes). Let $\{k_0\}$ be a set of lowest resonant frequencies, and $\{Q\}$ a set of the corresponding Q-factors, when a specimen is introduced in a cavity. $\{k_0\}$ and $\{Q\}$ depend on geometrical and electrical properties of the cavity - specimen set-up. To simplify analysis, only a set of geometrical parameters, $\{G\}$, and a set of electrical parameters, $\{P\}$, are considered. Two kinds of problems are then in order:

- Forward (Mode Analysis) Problem: Given $\{G\}$ and $\{P\}$ of the specimen, Find $\{k_0\}$ and $\{Q\}$.
- Inverse (Reconstruction) Problem: Given $\{k_0\}$ and $\{Q\}$, Reconstruct Parameter(s) in $\{G\}$ and $\{P\}$.

Both problems are considered in this paper, with emphasis on the mode analysis. Various methods can be used for this characterization. Analytical tools are useful only when separation of variables is posssible [1,2]. Numerical methods have to be invoked in any other case. Among these methods, mode matching [3], integral equation method [2,4] and null field method (eigenfunction expansions and boundary condition matching) [5] are frequently used. These methods usually involve complex, full matrices. In addition, these matrices are functions of resonant frequencies; therefore, iterative methods have to be used to search the zeros [5].

In this paper, a numerical model for the characterization of materials is proposed. Unlike the cavity perturbation method, the insertion here can be of arbitrary size and shape. This model uses the recently established finite "edge" element method with divergence free shape functions to discretize the vector eigenvalue problem. It has the advantage of accurately computing the eigenmodes and eliminating nonphysical modes that commonly occur in the finite element analysis of cavity problems. The paper is

Review of Progress in Quantitative Nondestructive Evaluation, Vol. 10A
Edited by D.O. Thompson and D.E. Chimenti, Plenum Press, New York, 1991

organized as follows. First, the theoretical basis is briefly introduced. Then, the finite element method is applied to obtain various eigenvalue systems based on material properties. After briefly describing the numerical model, we give some representative examples of characterizing specimens when various parameters are varied. An example of reconstruction is also given.

THEORETICAL BASIS

The problem under consideration is to find the resonant frequencies and the corresponding field distributions in a microwave cavity containing a test specimen. With $e^{j\omega t}$ variation implied, the modes in the cavity must be the solution of one of the following $curlcurl$ equations:

$$\nabla \times \frac{1}{\mu_r} \nabla \times \vec{\mathbf{E}} - k_0^2 \epsilon_r^{'}(\vec{\mathbf{r}}) \vec{\mathbf{E}} \;=\; \vec{\mathbf{0}}, \tag{1}$$

$$\nabla \times \frac{1}{\epsilon_r^{'}(\vec{\mathbf{r}})} \nabla \times \vec{\mathbf{H}} - k_0^2 \mu_r \vec{\mathbf{H}} \;=\; \vec{\mathbf{0}}, \tag{2}$$

Let L be a spatial scaling factor, the free-space wave number and the complex relative permittivity are given by

$$k_0 = L\omega\sqrt{\mu_o \epsilon_0}, \quad \epsilon_r^{'} = \epsilon_r(1 - j\tan\delta). \tag{3}$$

The loss tangent is related to the imaginary part of dielectric constant and conductivity of the material via

$$\tan\delta = \frac{\epsilon_r^{"}}{\epsilon_r} + \frac{\sigma\eta_0}{k_0\epsilon_r}, \quad \eta_0 = \sqrt{\mu_0/\epsilon_0}. \tag{4}$$

At microwave frequencies, the first part is dominant. Typically, ϵ_r is constant and $\epsilon_r^{"}$ increases with frequency [1,2]. Throughout the paper, k_0 $(rads/m)$ is treated as the resonant frequency for numerical convenience. On material interfaces, $\vec{\mathbf{E}}$ and $\vec{\mathbf{H}}$ must be tangentially continuous.

To obtain numerical solutions to (1) and (2), it is advantageous to consider their weak forms: for $\vec{\mathbf{E}}$ formulation,

$$\iiint_\Omega \left(\frac{1}{\mu_r}\nabla \times \vec{\mathbf{E}}\right) \cdot (\nabla \times \vec{\mathbf{w}}_m) d\Omega - k_0^2 \iiint_\Omega \epsilon_r^{'}(\vec{\mathbf{r}}) \vec{\mathbf{E}} \cdot \vec{\mathbf{w}}_m d\Omega$$

$$= jk_0\eta_0 \iint_S \left(\hat{\mathbf{n}} \times \vec{\mathbf{H}}\right) \cdot \vec{\mathbf{w}}_m dS, \tag{5}$$

and for $\vec{\mathbf{H}}$ formulation,

$$\iiint_\Omega \left(\frac{1}{\epsilon_r^{'}(\vec{\mathbf{r}})}\nabla \times \vec{\mathbf{H}}\right) \cdot (\nabla \times \vec{\mathbf{w}}_m) d\Omega - k_0^2 \iiint_\Omega \mu_r \vec{\mathbf{H}} \cdot \vec{\mathbf{w}}_m d\Omega$$

$$= -\frac{jk_0}{\eta_0} \iint_S \left(\hat{\mathbf{n}} \times \vec{\mathbf{E}}\right) \cdot \vec{\mathbf{w}}_m dS, \tag{6}$$

where $\vec{\mathbf{w}}_m$ is any set of real vector weighting functions. When the tangential components are used as unknowns, these weak forms are extremely useful in the following sense. First of all, it is simple to impose boundary conditions. In the $\vec{\mathbf{E}}$ formulation, a natural boundary condition, $\hat{\mathbf{n}} \times \vec{\mathbf{H}} = 0$, is automatically satisfied; a homogenous boundary

condition, $\hat{\mathbf{n}} \times \vec{\mathbf{E}} = 0$, can be imposed separately. Similarly in the $\vec{\mathbf{H}}$ case, $\hat{\mathbf{n}} \times \vec{\mathbf{H}} = 0$ is a homogenous condition , and $\hat{\mathbf{n}} \times \vec{\mathbf{E}} = 0$ is a natural condition. Second, it is easy to employ symmetry conditions. For example, when it is required to compute a mode where the electrical field is symmetrical to a plane, one can simply set a natural condition $\hat{\mathbf{n}} \times \vec{\mathbf{H}} = 0$ on the plane. Third, these weak forms allow one to take into account the large but finite conductivity in the cavity wall, since an impedance boundary condition [1] can be introduced in the surface integral in the weak form. The impedance boundary condition, however, is not considered in the present paper; instead, a perfectly conducting condition is assumed on the cavity wall. Since (5) and (6) are dual to each other, one needs to solve only one of them. However, they may yield eigenvalue systems of different types, depending on material properties. They also yield eigenvalue systems of different sizes, when boundary and symmetry conditions are imposed. Thus, one may choose $\vec{\mathbf{E}}$ or $\vec{\mathbf{H}}$ as the state variable according to particular problems.

FINITE ELEMENT COMPUTATION OF EIGENMODES

To solve (6) in infinite dimensions is practically impossible. In this section, the finite element method is used to map the eigenproblem into finite dimensions. It is well known that the standard (node based) finite element solution to the vector eigenvalue problem (2) contains both physical and nonphysical solutions. One obvious reason is that one is directly solving the *curlcurl* equation, leaving the divergence free condition, $\nabla \cdot \vec{\mathbf{H}} = 0$, unspecified. Therefore, the penalty method and reduction method were introduced to force this condition (see [6,7] and the reference cited therein). In this work, we use the linear "edge" finite elements built on a tetrahedral model. The six vector shape functions in a tetrahedron element are

$$\vec{\mathbf{w}}_n(\vec{\mathbf{r}}) \;=\; sgn(n)\frac{l_n}{\delta}\left(\vec{\mathbf{p}}_{7-n,1} \times \vec{\mathbf{p}}_{7-n,2} + \vec{\mathbf{e}}_{7-n} \times \vec{\mathbf{r}}\right), \tag{7}$$

where $n = 1, 2, \cdots, 6$, and other quantities are defined in [8]. These functions possess zero divergence. By introducing the following expansion

$$\vec{\mathbf{H}}(\vec{\mathbf{r}}) = \sum_{n=1}^{M} H_n \vec{\mathbf{w}}_n(\vec{\mathbf{r}}) \tag{8}$$

where H_n are the tangential components of $\vec{\mathbf{H}}$ along edges, $\vec{\mathbf{H}}$ is divergence free within the cavity and tangentially continuous on material interfaces. Thus, spurious modes due to non-divergence are deleted, and no special treatment is needed on material interfaces, which significantly simplifies the analysis.

With the vector weighting functions chosen to be the same as the shape functions (7), (6) is reduced to a generalized algebraic eigenvalue problem:

$$\left([A(k_0)] - k_0^2[B]\right)\;\{H\} \;=\; 0. \tag{9}$$

where $[A(k_0)]$ depends on k_0, and it can be evaluated only when k_0 is given. However, one observes that (9) has a nonzero solution only if the determinant of the stiffness matrix is zero:

$$\det(R) = \det\left([A(k_0)] - k_0^2[B]\right) \;=\; 0. \tag{10}$$

Thus, the problem becomes one of searching the zeros of (10) in the complex plane [5]. In the case where the loss tangent does not vary with frequency, (9) becomes a complex algebraic eigensystem. When no loss is present, a real, symmetrical system is obtained.

In contrast to the $\vec{\mathbf{H}}$ formulation, the $\vec{\mathbf{E}}$ formulation gives an explicit expression:

$$\left([A] - k_0^2[B] + jk_0[C] - jk_0^3[D]\right) \{E\} = 0, \tag{11}$$

where matrix $[C]$ is due to nonzero conductivities, and $[D]$ is due to the fact that ϵ'' is proportional to frequency. Equation (11) can be reduced into a real, unsymmetrical eigensystem of triple size:

$$\begin{bmatrix} A & 0 & 0 \\ 0 & B & 0 \\ 0 & 0 & D \end{bmatrix} \begin{Bmatrix} E \\ \lambda E \\ \lambda^2 E \end{Bmatrix} = \lambda \begin{bmatrix} -C & -B & D \\ B & 0 & 0 \\ 0 & D & 0 \end{bmatrix} \begin{Bmatrix} E \\ \lambda E \\ \lambda^2 E \end{Bmatrix}, \tag{12}$$

where $\lambda = jk_0$. In the case where $\epsilon_r'' = 0$, Equation (11) can be reduced into a real, unsymmetrical eigensystem of double size:

$$\begin{bmatrix} A & 0 \\ 0 & B \end{bmatrix} \begin{Bmatrix} E \\ \lambda E \end{Bmatrix} = \lambda \begin{bmatrix} -C & -B \\ B & 0 \end{bmatrix} \begin{Bmatrix} E \\ \lambda E \end{Bmatrix}. \tag{13}$$

And finally, when no loss is present, a simple real, symmetrical system is obtained: $[A]\{E\} = k_0^2[B]\{E\}$.

Once the solutions are available, the Q-factors can be computed using eigenvectors through the following definition

$$Q = \omega \frac{\text{Energy Stored in the Cavity}}{\text{Dielectric Losses} + \text{Metal Wall Losses}}. \tag{14}$$

The stored energy and the dissipated power in the cavity can be computed using the vector shape functions and the FEM solutions.

One shortcoming of using FEM to solve the vector eigenproblem, compared to the eigenfunction expansion type methods, is that the mode index information is lost. For a complicated geometric configuration, mode classification can be difficult, sometimes impossible. In practice, cavities and specimens may be manufunctured and arranged in such a way , that the commonly used definitions for cavity modes (such as TE_{mnl}, TM_{mnl}, Hybrid, etc.) are still applicable. Under such a circumstance, the mode information may be retrieved by checking the eigenvectors. This can be realized in two steps: 1) identify mode type (TE, TM, etc.); 2) identify mode index (m, n, l). The second step is usually more difficult. In addition, applying symmetry and anti-symmetry conditions may separate some modes and facilitate mode identifications, and at the same time, significantly reduce the size of the eigenproblem.

DESCRIPTION OF THE NUMERICAL MODEL

A computer code for research purpose has been writtern based on the previous discussion. It contains the following five basic building blocks: 1) Geometrical Descriptor, 2) Mesh Generator, 3) Matrix System Assembler, 4) EigenSystem Solver, and 5) Multi-Purpose Post-Processor. In this work, the sparse eigenvalue code "STLM" (spectral transformation Lanczos method [9]) is used to solve the matrix system for lossless problems. This code requires skyline storage, and thus can handle relatively large models if the bandwidth is minimized. The real and complex QZ algorithms (available in EISPACK) are used to solve various matrix systems for lossy cavity problems. These codes require full matrix storage, and thus can only handle small sized models. In the literature, Lanzcos algorithm [10] and subspace iteration method [11] have been used to solve a real

gyroscopic eigensystem. The numerical performances of these methods for the present model are under study. To be added to the post-processor is a model identification program, as identifying modes in a finite element eigenvalue solution remains an open question in this work.

These basic modules are then linked appropriately for both forward (model analysis) and inverse (reconstruction) problems. In a forward set-up, the five modules are called consecutively for each change in geometrical parameters; the geometrical descriptor and mesh generator are called only once if only electrical parameters are changed. In an inverse set-up, it is assumed that the resonant frequencies and the corresponding Q-factors are measured, and an interval containing the parameter to be reconstructed is known. The Regula Falsi method is invoked to search the required point iteratively.

NUMERICAL EXAMPLES

The sets $\{G\}$ and $\{P\}$ cover a wide range of parameters. In most practical situations, it is of interest to see how the resonant frequencies vary with one or two parameters in the sets. In this section, some typical examples are given, where the cavities are of simple shapes and isotropically loaded. The first example is a rectangular specimen $(0.125m \times 0.175 \times 0.1m)$ loaded on the bottom center of a rectangular cavity $(0.5m \times 0.3 \times 0.2)$. $\vec{\mathbf{H}}$ is chosen as the state variable. Only one-quarter of the geometry is used. On the planes $x = 0$ and $y = 0$, $\hat{\mathbf{n}} \times \vec{\mathbf{H}} = 0$ is assumed. On the remaining surface, $\hat{\mathbf{n}} \times \vec{\mathbf{E}} = 0$ is applied. Fig. 1 shows the mode chart when the dielectric constant of the specimen is varied. It is interesting to observe that in this case, modes do not intersect each other.

The second example is a dielectric sphere (Radius $= 0.5m$) concentrically loaded in a spherical cavity (Radius $= 1m$). Only one-eighth of the geometry is considered. Fig. 2 shows the variation of resonant frequencies with the dielectric constant of the specimen. The four modes denoted by triangles and the three modes denoted by circles are obtained

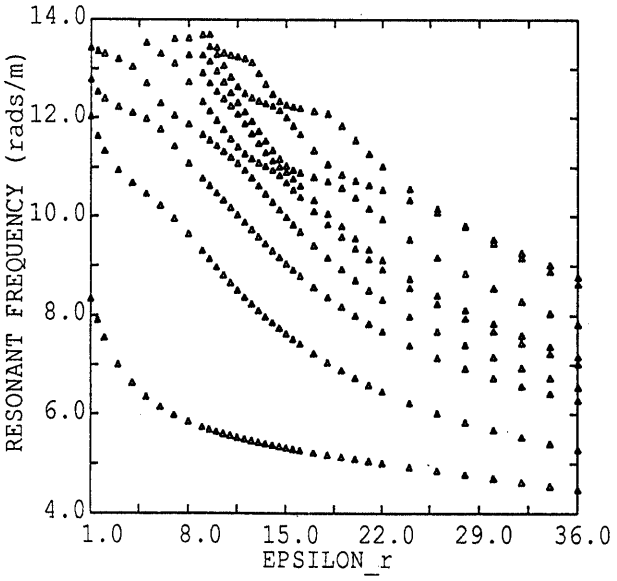

Fig.1 Mode chart of a rectangular specimen in a rectangular cavity.

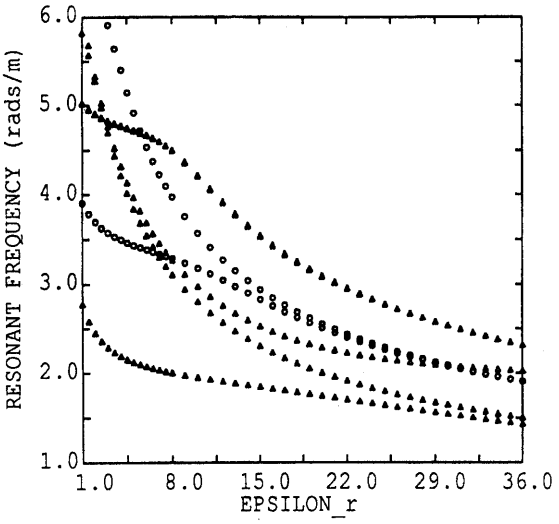

Fig.2 Mode chart of a concentric sphere in a spherical cavity.

by different combinations of symmetry conditions. It can be seen that tracking of modes is rather complicated, since different modes have different sensitivities to a change in the dielectric constant.

The third example is a dielectric sphere (Radius = $0.18m$) with $\epsilon_r = 36$ *eccentrically* loaded in a spherical cavity (Radius $=1m$). Two way symmetry is employed. Fig. 3 shows the mode chart when the eccentricity is changed. We see that Hybrid modes other than TE and TM show up as the specimen is shifted off center.

In some cases, one may be interested only in the dominant mode. The fourth example is a cubic specimen at the center of a spherical cavity (Radius $=1m$). Fig. 4

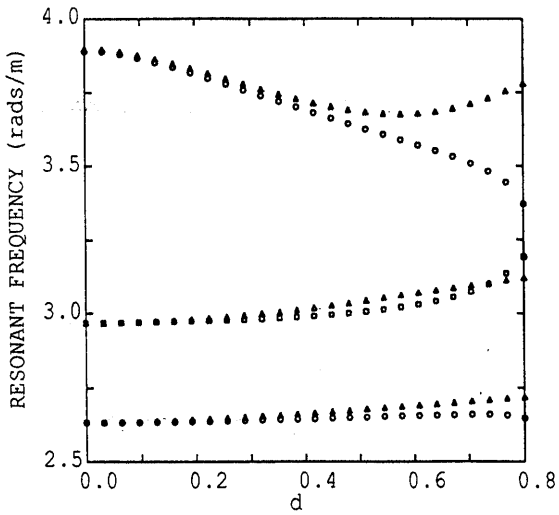

Fig.3 Mode chart of an eccentric sphere in a spherical cavity.

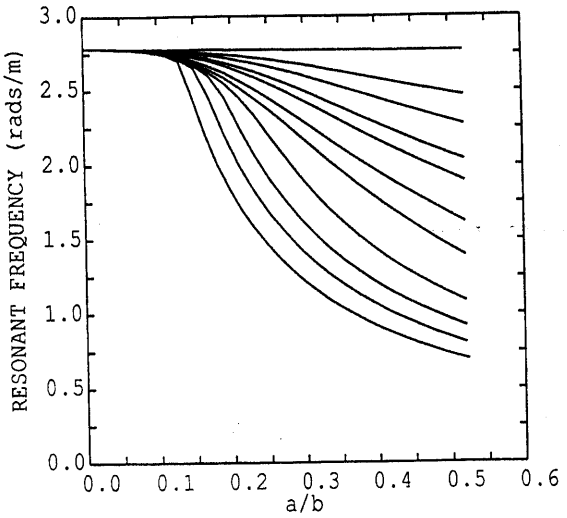

Fig.4 Doninant mode chart of a concentric cube in a spherical cavity.

shows the variation of the dominant mode with the size (a/b is the ratio of half side length of the cube to the radius of cavity) and dielectric constant of the cube. The family of curves correspond, vertically, to ϵ_r = 1,1.5,2,3,4,8,15,36, 54,72,98.

The last example is a spheroid at the center a cylindrical cavity. The dielectric constant of the spheroid is assumed to be a linear function of water content c: $\epsilon_r = 9 + 70 \cdot c$. The problem here is to reconstruct the dielectric constant, provided that the resonant frequencies are measured. First, the k_0 of the lowest TE mode corresponding to different water contents is computed. To simulate measurement data, some random noise is added to the computed data. The Regula Falsi method converges in 4 to 5 iterations in this case. Fig. 5 shows the noise added resonant frequencies, and Fig. 6 shows the reconstructed results, where the solid line stands for ideal curves; circles and triangles correspond to 1% and 5% random noise, respectively. Good predictions are observed.

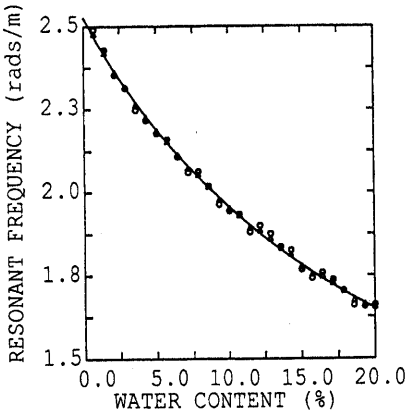

Fig.5 Noise included k_0.

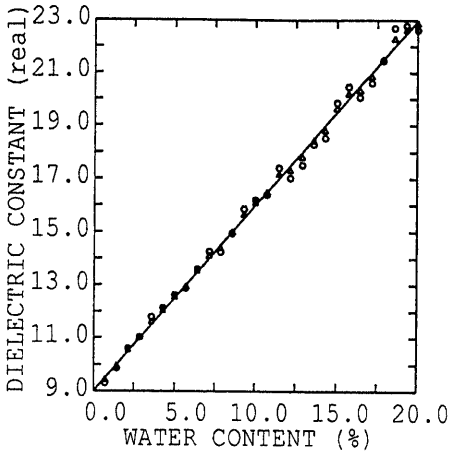

Fig.6 Reconstructed ϵ_r.

SUMMARY

A numerical model using FEM was built to characterize specimens in microwave cavities. No spurious modes were observed in the interested range. For some simple geometries, the model can predict the lowest modes with satisfatory accuracy. Various curves were computed. In some cases, reconstruction is possible. Future work will address the following: efficient eigen codes for large, sparse complex and real non-symmetric systems; rigorous mode identification in FEM solutions; more realistic applications; and characterization of anisotropic specimens.

ACKNOWLEDGMENT

This work was supported in part by NSF Grant #EET8714628. Computational Resources on a CRAY Y-MP were provided by the Ohio Supercomputer Center. The "STLM" code was provided by Thomas Ericsson, Department of Computer Science, Chalmers University of Technology, Sweden.

REFERENCES

1. R. E. Collin, Foundations for Microwave Engineering, McGraw-Hill Book Company, 1966, pp.36-37.
2. D. Kajfez and P. Guillon (eds), Dielectric Resonators, Artech House Inc., 1986.
3. A. Julien and P. Guillon, IEEE Trans. Microwave Theory Tech. MTT-34, 723, 1986.
4. D. Kajfez, A. W. Glisson and J. James, IEEE Trans. Microwave Theory Tech. MTT-31, 1023, 1983.
5. W. Zheng, IEEE Trans. Antennas Propagat. AP-37, 1732, 1989.
6. J. P. Webb, IEEE Trans. Microwave Theory Tech. MTT-33, 635, 1985.
7. J. P. Webb, IEEE Trans. Magnetics MAG-24, 162, 1988.
8. M. L. Barton and Z. J. Cendes, J. Appl. Phys. 61, 3919, 1987.
9. T. Ericsson and A. Ruhe, Math. Comput. 35, 1251, 1980.
10. O. A. Bauchau, Int. J. Numer. Meth. Eng. 23, 1705, 1986.
11. J. F. D. Rodrigues and T. E. C. Gmuer, Int. J. Numer. Meth. Eng. 28, 511, 1989.

Review of Progress in

QUANTITATIVE NONDESTRUCTIVE EVALUATION

Volume 10A